J 2.12   CONSTRAINING CIRRUS ICE CRYSTAL SIZE THROUGH

OBSERVATION OF HALOS

Margaret B. Kimball[1],Timothy J. Garrett[*]

[1]University of Utah, Salt Lake City, Utah

1 INTRODUCTION

It has been argued that ice crystals can shatter on the inlets of such instruments as the Forward Scattering Spectrometer Probe (FSSP) and Cloud Integrating Nephlometer (CIN), artificially inflating measurements of concentration and extinction coefficient (Gardiner and Hallett 1985; Gayet et al. 1996; Heymsfield et al. 2006). Several prior studies have used cirrus optics to visually determine ice crystal characteristics. For example, Riikonen et al. (2000) used instances of rare halo phenomena to argue for the existence of cubic ice in the earth's atmosphere. Here we propose that cirrus optical effects can also provide a means for independently assessing ice crystal size, thereby constraining the extent of errors in in situ observations.

The Mid-Latitude Cirrus Experiment (MidCiX) took place over the central plains of the US and the Gulf of Mexico in April and May 2004. It comprised 9 flights by the NASA WB-57F high altitude aircraft based from Houston, TX. The WB-57F was equipped to measure ice particle characteristics using a multitude of cloud probes. MidCiX provided an excellent opportunity to examine the relationship between cirrus optical effects and ice crystal properties. While flying in high altitude cirrus, halos were noted by the WB-57F back seater. Because the plane was near cloud top, multiple-scattering contributions to observed down-welling radiances were low, and a strong correlation between in-situ measurement of ice crystal characteristics and single-scattering opti-

cal phenomena could be drawn.

2 THEORY

The lower ice crystal size limit required for the formation of halos is governed not by crystal geometry, but rather by the wave nature of light. As the size of ice particles decreases relative to the wavelength of incident light, diffractive effects smooth out halo peaks (Fig 1 (a)). The equivalent radius (r_{eq}) a crystal would have if its cross sectional area were converted into a circle is used to examine the size restrictions for halo formation. The smallest size conducive to halo formation is r_{eq} between $7\ \mu$m and $11.6\ \mu$m (Fig 1 (a)). Similar results have been obtained by Mischenko and Macke (1999), who used T-matrix theory to show that 46 degree halos cannot form for size parameters <100 ($r_{eq} \leq\ O\ (10\mu$m) at visible wavelengths). The upper ice crystal size limit required for halo formation is determined by the nature of crystal growth. At cold temperatures, ($T \leq -20°C$), ice crystals grow such that as r_{eq} increases, their aspect ratio (width/height) decreases (Kobayashi 1961; Auer and Veal 1970). Less ice crystal surface area comprises the basal face, reducing the probability that randomly oriented crystals refract light in the manner required to form a 46 degree halo. Thus, it is estimated that the 46 degree halo has a significantly diminished likelihood of formation for ice crystals with $r_{eq} >\sim 100\mu m$ (Fig 1(b)). A second consideration is that larger crystals ($\geq 100\mu m$) are less likely to fall with the random orientation required for halo circular symmetry. (Sassen 1980; Tape 1994)

[*]*Corresponding author address:* Timothy J. Garrett, 135 S 1460 E, Room 819 Salt Lake City, UT 84112-0110; e-mail: tgarrett@met.utah.edu

Figure 1: Phase function for column crystals of various sizes.
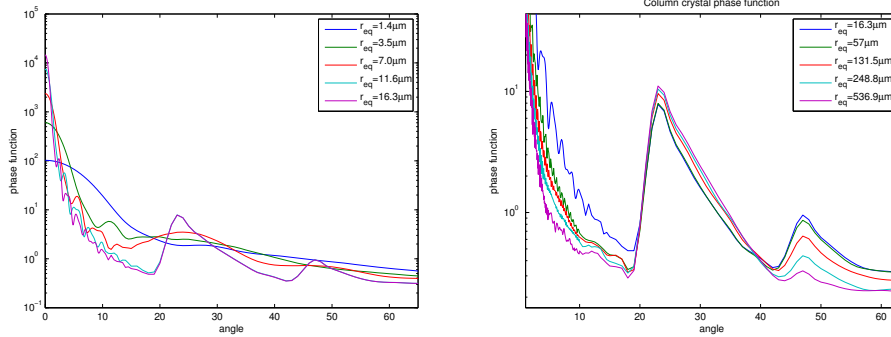
(a) 46 degree halo washes out for small particles (b) 46 degree halo dissapears for large particles

3 OBSERVATIONS

3.1 Instrumentation

The WB-57F was equipped with three size distribution probes: a Cloud Particle Imager (CPI), a FSSP-100, and a Cloud Aerosol and Precipitation Spectrometer (CAPS). The CPI imaged particles from 10 to 750 μm and provides information on the shape of ice crystals. The FSSP measured particles between 2 and 50 μm. The CAPS was comprised of two instruments, the Cloud and Aerosol Spectrometer (CAS) and the Cloud Imaging Probe (CIP) which collectively measured particles between 1 and 1600 μm across (Baumgardner et al. 2002). In addition to the spectral probes, bulk ice water content was measured by the Harvard Ice Water Probe (Weinstock et al. 1994) and bulk optical extinction measurements were obtained from the CIN (Gerber et al. 2000).

3.2 Halos

Halo observations were determined from when the flight notes from the backseater in the WB-57F noted a "double halo" or a "46 degree halo". Microphysical and environmental characteristics during the halo sightings were calculated as a 1 min average centered on the halo observation times. Photographs (e.g. Fig 2) provided visual confirmation. Not all 46 degree halos were noted or photographed. However, a total of six 46 degree halos and twenty 22 degree halos were recorded during MidCiX. Further, the back-seater estimated that in fact halos were present about half of the time the WB-57F was in cloud and near cloud-top, and less often deeper in the cloud, presumably due to the smoothing effects

Figure 2: Photograph of concentric halos during MidCiX

of multiple-scattering.

3.3 Cloud Properties

Environmental and bulk cloud properties were calculated for the average of all halo sightings during MidCiX; the average temperature was $T = -41 \pm 6.2°C$, ice water content $IWC = 0.016 \pm .013 \ gm^{-3}$, optical extinction β_{ext}=1.7 $\pm$ 0.7 km^{-1}, and area equivalent radius r_{eq} =14.9 $\pm$ 3.7μm from the CIN. Fig 3 shows the averaged normalized distributions of cross sectional area and number concentrations from the CAPS probes in a 1 min window centered around halo observation times and as the average for all MidCiX flights. There are two distinct modes in the distributions, one at $r_{eq} \approx 10\mu m$ and a second at $r_{eq} \approx 100\mu m$. The smaller mode dominates the concentrations of both quantities. While the bimodality might reflect a true cloud and precipitation mode in the cirrus cloud, it may be argued instead

Figure 3: Normalized Area (green) and Number (blue) concentration distributions from the CAPS probes for 46 degree halo sightings (dashed) and MidCiX mean (solid).
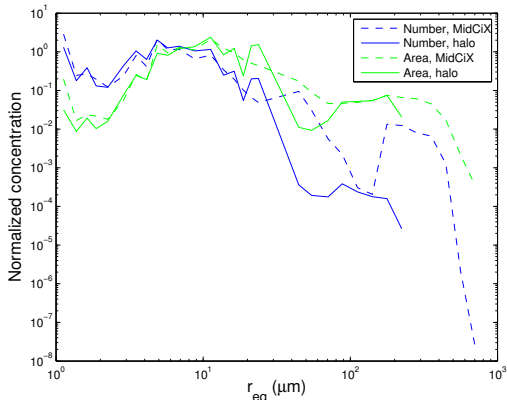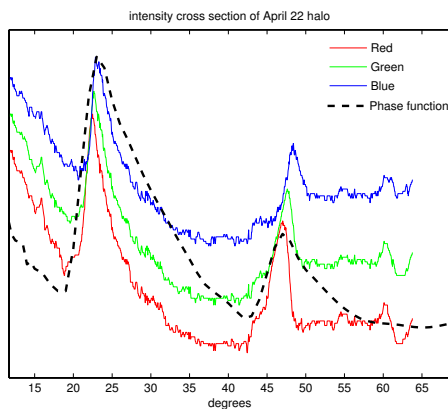

Figure 4: Brightness cross-section of image from April 22 with theoretical $16\mu m$ column crystal phase function

that the small mode is simply an artifact of precipitation mode shattering in the CAPS inlet. Halo observations can be used to discriminate between these two hypotheses.

3.4 Case Study

The photograph (Fig 2) depicts both the 22 and 46 degree halos. It was taken from the WB-57F on April 22, 2004 at 18:30 local time while the aircraft was flying in cirrus over the Gulf of Mexico. Assuming Fig 2 illustrates scattering in the single-scattering regime, the ice crystal phase function may be found directly by taking an intensity cross-section across the digital image. The red, green, and blue components each show two halos. For comparison the theoretical phase function, for red light ($\lambda = 650nm$) for $r_{eq} = 16\mu m$ column crystals was super imposed on the brightness cross section. An assumption is made that peaks in photograph intensity correspond to the 22 degree and 46 degree halos. To extract the angular distribution of transmitted intensity, a reference value is needed. A minimum in intensity occurs at approximately 40 degrees from the sun, where cloud scattering is particularly low. Clear sky intensity at this zenith angle is calculated using the Streamer radiative transfer code (Key and Schweiger 1998) specifying the date, time, location, and height of the aircraft at the time of the halo sighting. The calculated blue sky intensity ($8.5 \; \mathrm{Wm}^{-2}\mathrm{sr}^{-1}$) is then used to scale intensities for the rest of the image.

In general, the relationship between transmittance and intensity is defined by

$$T(\mu) = \frac{\pi I(\mu)}{\mu_0 F_0} \qquad (1)$$

where T is the transmittance (unit less) at observer angle μ, μ_0 is the cosine of the solar zenith angle, $I(\mu)$ is the observed intensity, and F_0 is the solar constant. Using this relationship, the cloudy transmittance at 46 degrees from the sun in Fig. 4 is found to be 0.0308. Assuming the observed intensity distribution lies in the single-scattering regime, an order of magnitude estimate for the optical depth of the cloud that produced the halo at angle $\mu' = \cos(46 \text{ degrees})$ is (Liou, 2002)

$$\Delta\tau = \frac{T(\mu' + \mu_0, \mu_0)}{P(\mu' + \mu_0, \mu_0)} 4(\mu' + \mu_0) \cdot \mu_0 \qquad (2)$$

Where $P(\mu' + \mu_0, \mu_0)$ is the ice crystal phase function. Using the transmittance established from Eq. (1), and combining it with the value of the theoretical phase function at 46 degrees, we then estimate from Eq. (2) that the optical depth of cloud above the aircraft is $\Delta\tau \approx 1.2$.

A comparison is now made between the physical cloud depth required to obtain the value of $\Delta\tau$ to the extinction contributions from the cloud and precipitation modes of the measured ice crystal distributions (Fig 3.3). Integrated particle β_{ext} for precipitation sized particles ($r_{eq} \geq 50\mu m$) during halo sightings was 0.09 km^{-1}, while β_{ext} for cloud particles ($r_{eq} \leq 50 \; \mu m$) was 1.93 km^{-1}. Thus, a cloud depth of 13 km above the aircraft would be required for suf-

ficient scattering to form a halo were only precipitation particles present. If, however the cloud mode of ice crystals is considered, a depth of only 0.6 km is required. Since the WB-57F was flying at cloud top when these observations were obtained, cloud mode ice crystals appear necessary to account for the observations. In their absence, the cloud top would need to extend well into the middle stratosphere.

4 SUMMARY

Theoretical considerations imply that the formation of 46 degree halos requires that the area equivalent radius of ice crystals must be greater than $\sim 10\ \mu$m to eliminate diffraction effects, but smaller than $\sim 100\ \mu$m for significant scattering to occur through a basal face. Applying these restrictions to the MidCiX size distributions during times when halos were observed (Fig 3), it is apparent that halos cannot form from precipitation mode ice crystals and thus cloud mode ice crystals must dominate the cloud optical properties.

Further, analysis of a photograph taken during the flights demonstrates that measured cloud mode ice crystals have sufficiently dense scattering cross-sections to account for observed halo intensities whereas precipitation sized ice crystals do not. The implication is that optical extinction during the time periods of halo observations was dominated by a real cloud mode of ice crystals that could not be attributed to shattering of precipitation mode crystals alone.

The importance of cirrus to global climate necessitates accurate parameterization of ice crystal size. We have shown that visual observations of halos can constrain the prevalence of small ice crystal measured by cloud probes. Observations of halos from amateur cloud photographers may contribute to a more coherent global picture of cirrus radiative properties.

5 BIBLIOGRAPHY

Auer, A.H. and D.L. Veal, 1970: The Dimension of Ice Crystals in Natural Clouds. *J. Atmos. Sci*., **27,** 919-926.

Baumgardner, D., H. Jonsson, W. Dawson, D. O'Connor, and R. Newton, 2002: The cloud, aerosol and precipitation spectrometer (CAPS): A new instrument for cloud investigations. *Atmos. Res.*, **59-60**,251-264.

Gardiner, B.A. and J. Hallett, 1985: Degradation of In-Cloud Forward Spectrometer Probe measurements in the presence of Ice Particles. *J. Atmos. Ocn. Tech.*, **2**, 171-181.

Gayet, J., G. Febvre, and H. Larsen, 1996: The reliability of the PMS FSSP in the presence of small ice crystals. *J. Atmos. Oceanic. Technol.*, **13**, 1300-1310.

Gerber, H., Y. Takano, T.J. Garrett, P. Hobbs, 2000: Nephlometer measurements of the asymmetry parameter, volume extinction coefficient and backscatter ratio in cloud. *J. Atmos. Sci.*, **57**, 3021-3034.

Heymsfield, A.J., C. Schmitt, A. Bansemer, G. van Zadelhoff, M.J. McGill, C. Twohy, D. Baumgardner, 2006: Effective radius of ice cloud particle populations derived from aircraft probes. *J. Atmos. Oceanic Technol.*, **23**, 361-380.

Key, J. and A. Schweiger, 1998: Tools for atmospheric radiative transfer: Streamer and FluxNet. *Computers and Geoscience*, **24**, 443-451.

Kobayashi, T. 1961: The growth of ice crystals at low supersaturations. *Philosophical Magazine*, **6**, 1363-1370.

Liou, K.N., 2002. *An Introduction to Atmospheric Radiation*. Academic Press, 583pp.

Mischenko, M. I. and A. Macke, 1999: How big should hexagonal crystals be to produce halos?, *Applied Optics,* **38**, 1626-1629.

Riikonen, M., M. Sillanpaa, L. Virta, D. Sullivan, J. Moilanen, I. Luukkonen, 2000: Halo observations provide evidence of airborne cubic ice in the Earth's atmosphere. *Applied Optics*, **39**, 6080-6085.

Sassen,K., 1980: Remote Sensing of planar ice crystal fall attitudes. *J. Meteor. Soc. Japan*, **58**, 422-429.

Tape, W., 1994. *Atmospheric Halos,* Antarctic Research Series, 164pp.

Trankle, E. and R.G. Greenler, 1987: Multiple-scattering effects in halo phenomena. *J. Opt. Soc. Am. A.*, **4**, 591-599.

Weinstock, E.M., E.J. Hintsa, A.E. Dessler, J.F. Oliver, N.L. Hazen, J.N. Demusz, N.T. Allen, L.B. Lapson, J.G. Anderson, 1994: New fast response photofragment fluorescence hygrometer for use on the NASA ER-2 and Perseus remotely piloted aircraft. *Rev. Sci. Instrum.*, **65**, 3544-3554.